Computer Methods and Programs in Biomedicine 188 (2020) 105296

Contents lists available at ScienceDirect

Computer Methods and Programs in Biomedicine

journal homepage: www.elsevier.com/locate/cmpb

Classification model based on strain measurements to identify patients with arrhythmogenic cardiomyopathy with left ventricular involvement

Yolanda Vives-Gilabert[a,*], Esther Zorio[b,c,d,*], Jorge Sanz-Sánchez[b,c], Pilar Calvillo-Batllés[e], José Millet[a,c], Francisco Castells[a]

[a] Instituto ITACA, Universitat Politècnica de Valencia, Camino de Vera s/n,València 46022, Spain
[b] Unidad de Cardiopatías Familiares, Muerte Súbita y Mecanismos de Enfermedad (CaFaMuSMe), Instituto de Investigación Sanitaria La Fe, Avenida Fernando Abril Martorell no. 106, Valencia, Spain
[c] Unidad de Valoración del Riesgo de Muerte Súbita Familiar, Servicio de Cardiología, Hospital Universitario y Politécnico La Fe, Valencia, Spain
[d] Center for Biomedical Network Research on Cardiovascular Diseases (CIBERCV), Madrid, Spain
[e] Servicio de Radiología, Hospital Universitario y Politécnico La Fe, Valencia, Spain

ARTICLE INFO

Article history:
Received 22 March 2019
Revised 22 November 2019
Accepted 21 December 2019

Keywords:
Cardiac magnetic resonance imaging
Clustering
Naïve Bayes classification

ABSTRACT

Background and objective: A heterogenous expression characterizes arrhythmogenic cardiomyopathy (AC). The evaluation of regional wall movement included in the current Task Force Criteria is only qualitative and restricted to the right ventricle. However, a strain-based approach could precisely quantify myocardial deformation in both ventricles. We aim to define and modelize the strain behavior of the left ventricle in AC patients with left ventricular (LV) involvement by applying algorithms such as Principal Component Analysis (PCA), clustering and naïve Bayes (NB) classifiers.

Methods: Thirty-six AC patients with LV involvement and twenty-three non-affected family members (controls) were enrolled. Feature-tracking analysis was applied to cine cardiac magnetic resonance imaging to assess strain time series from a 3D approach, to which PCA was applied. A Two-Step clustering algorithm separated the patients' group into clusters according to their level of LV strain impairment. A statistical characterization between controls and the new AC subgroups was done. Finally, a NB classifier was built and new data from a small evolutive dataset was predicted.

Results: 60% of AC-LV patients showed mildly affected strain and 40% severely affected strain. Both groups and controls exhibited statistically significant differences, especially when comparing controls and severely affected AC-LV patients. The classification accuracy of the strain NB classifier reached 82.76%. The model performance was as good as to classify the individuals with a 100% sensitivity and specificity for severely impaired strain patients, 85.7% and 81.1% for mildly impaired strain patients, and 69.9% and 91.4% for normal strain, respectively. Even when the severely affected LV-AC group was excluded, LV strain showed a good accuracy to differentiate patients and controls. The prediction of the evolutive dataset revealed a progressive alteration of strain in time.

Conclusions: Our LV strain classification model may help to identify AC patients with LV involvement, at least in a setting of a high pretest probability, such as family screening.

1. Introduction

Arrhythmogenic cardiomyopathy (AC) is regarded as a primary myocardial disease with a low prevalence. Its characteristic progressive fibro-fatty myocardial infiltration may promote systolic ventricular dysfunction and ventricular electrical instability [18]. The variable phenotype (in terms of penetrance and expressivity) in patients with AC [20] make its diagnosis challenging. The current Task Force Criteria (TFC) comprise major and minor criteria sets in different categories [10,11] but, since they were designed to detect classical AC forms (with isolated or predominant right

** Corresponding authors.
E-mail addresses: yovigi@upv.es (Y. Vives-Gilabert), zorio_est@gva.es (E. Zorio).

https://doi.org/10.1016/j.cmpb.2019.105296

ventricular involvement), left ventricular (LV) forms of the disease often remain unrecognized [18,19]. According to the literature, between 33% and 60% of the patients suffer from LV wall motion abnormalities, excluding septal hypokinesia [18,19]. The TFC consider regional right ventricular (RV) akinesia/dyskinesia or dyssynchronous RV contraction as a criterion for diagnosing AC. However, no technical indications are given, no threshold for the RV analysis are provided and no LV wall motion abnormalities are mentioned. Briefly, the detection of wall motion abnormalities merely comes down to a kind of subjective evaluation restricted to the right ventricle.

Strain quantifies myocardial deformation by considering the resting position and the maximal displacement [22]. Giving the fact that deformation can be analyzed in three directions, also three strain time series (namely, radial, circumferential and longitudinal) may be studied. To characterize the strain, researchers usually consider peak strain values [3,15,25]. However, relying on a punctual value could lead to errors due to spurious fluctuations of the strain time-series or due to the low time resolution from frame to frame. In this paper, the entire strain curves from each LV AHA segment (i.e. 16 segments if we consider all but the apex), obtained from cardiac magnetic resonance imaging are considered, to use the whole available information and exploit it in a more robust manner.

As cardiac cells contract rather synchronously, it is obvious that there will be a high redundancy between the strain curves at the different segments, so a first step for dimensionality reduction will be required. Principal Component Analysis (PCA) is a statistical procedure that eliminates redundant data from a dataset and condense the linearly uncorrelated information into a few variables called “principal components” [5,14]. The coefficient matrix represents the influence of the linear combination of the different principal components to each variable and give information about the heterogeneity of the variables in terms of amplitude and shape of the time series. The coefficients associated to the first component could be used to characterize strain in AC patients with LV involvement.

Due to the wide variability in the phenotypic expression of the AC, we hypothesized that AC patients with LV involvement could manifest different patterns of LV strain. To investigate this effect, clustering techniques can be applied [7,16,24]. Clustering refers to the task of grouping a set of subjects in such a way that subjects in the same group (called a cluster) are more similar (according to their features) to each other than to those in other clusters. Therefore, AC patients with LV involvement could be divided into different clusters according to their degree of LV strain impairment.

Recently machine learning techniques are coming into use to analyze biomedical data: Support Vector Machines (SVM) [26], random forest [4], K-nearest neighbor (KNN) [23,29] or Bayesian classifiers [2,6,12], among others. Some of them have even been applied to cardiac strain measurements obtained from either echocardiography [13,21,23] or computed tomography [29]. Particularly, Bayesian classifiers have been successfully applied to solve heart related challenges [13] as well as to other biomedical problems, such as studies related to the brain [12]. Herein we will focus on Bayesian classifiers for the detection of strain impairment in the affected left ventricle of AC patients upon magnetic resonance imaging studies.

The aim of the present study is to further investigate LV strain impairment in patients diagnosed of AC with LV involvement, not in terms of quantitative differences when compared against controls as in our previous work [27], but in terms of patterns of dysfunction and clinical group prediction. Furthermore, the study was extended by applying Bayesian classifiers as an accurate automatic decision support system to detect strain impairment in new AC patients, the accuracy to discriminate controls and patients in the grey zone of strain performance was investigated and a novel evolutive strain data in the follow-up of a subset of these patients was provided. As far as we know, this is the first study that modelizes strain in arrhythmogenic cardiomyopathy patients with left ventricular involvement.

2. Materials and methods

2.1. Dataset

The sample comprised thirty-five patients diagnosed with AC with LV involvement (patients) and twenty-three relatives non-carriers of the pathogenic mutation of the proband (controls), all recruited in a specialized multidisciplinary referral unit focused on families with inherited cardiac diseases, and all included in our previous work [27]. Six of the 35 patients had 2 good quality CMRs in different time periods, between 1 and 5 years apart and were included in the evolutive dataset.

All subjects involved in this study were probands or proband’s relatives undergoing family screening, they all were mutation carriers and they all exhibited the typical LV subepicardial and/or intramyocardial pattern of late gadolinium enhancement which characterizes AC with LV involvement. Remarkably, all probands received an unequivocal AC diagnosis (with a ‘definite’ AC diagnosis following 2010 TFC criteria or with a histological confirmation at autopsy or at heart explant examination in patients undergoing heart transplantation). The ventricular predominance of the AC involvement (either RV, LV or biventricular) was assessed as previously reported [9]. Controls were family members in whom AC had been ruled out based on the cardiological work-up and did not carry the mutation identified in their affected relatives.

2.2. Magnetic resonance imaging and feature tracking

Patients and controls were scanned in a 1.5-Tesla scanner (Siemens Avanto, Siemens Symphony and GE Signa HDxt). Several cine long and short-axis slices were acquired as previously reported [27].

Strain parameters were calculated with the software Circle CVI^{42} version 5.5.1, Calgary, Canada. Semi-automated end-diastolic endocardial and epicardial limits of the left ventricle were traced in the three long axis and in the short axis cardiac chamber views (papillary muscles were excluded from the endocardial contour). The automated Circle tissue tracking algorithm yielded 3D strain curves in all the three directions for each of the LV American Heart Association (AHA) segments, excluding the apex (segment 17) as shown in Fig. 1.

Myocardial strain curves display the deformation of a myocardial segment in one of the following directions: radial, circumferential or longitudinal. It is defined as in equation below.

$$S(t_i) = \frac{L(t_i) - L(t_0)}{L(t_0)}, \tag{1}$$

where $L(t_i)$ is the radial, circumferential or longitudinal segment length at the i^{th} frame, being the initial frame at the end diastole, when the heart is fully expanded. A spline interpolation of the strain values was applied to have 101 time points.

Radial strain represents the radially directed myocardial deformation towards the center of the LV cavity and indicates the wall thickening during the systole. Circumferential strain derives from LV myocardial fiber shortening along the circular perimeter observed on a short-axis view. Finally, longitudinal strain represents the longitudinal shortening from the base to the apex. Since heart contraction implies some sort of wall thickening and cavity reduction, both circumferential and longitudinal strain are generally expressed by negative values, whereas radial strain is a

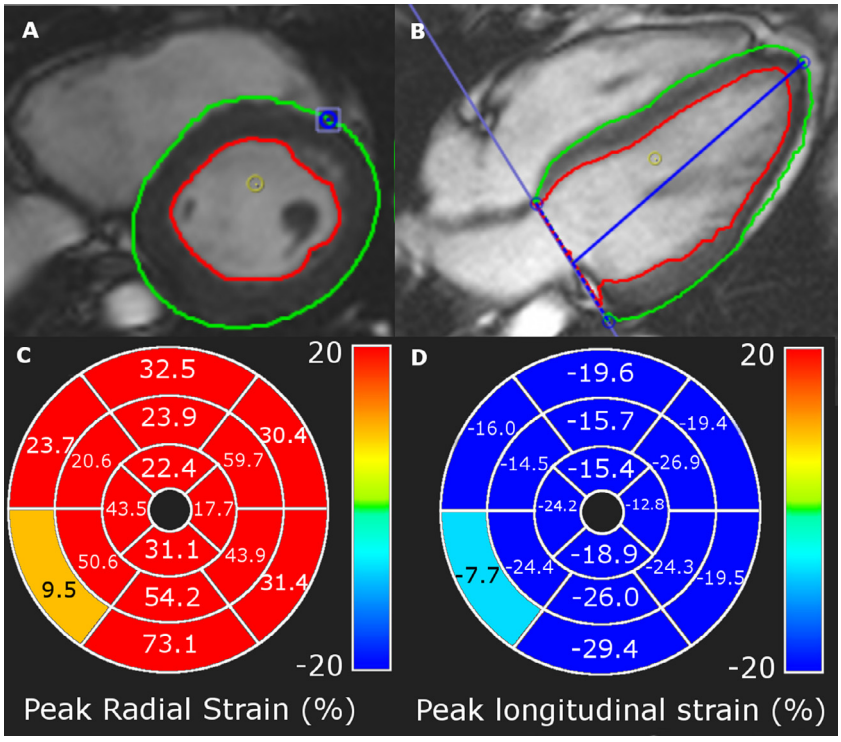

Fig. 1. Example of short axis (A) and long axis (B) delineation and results of peak strain in the 16 AHA segments for radial (C) and longitudinal (D) directions.

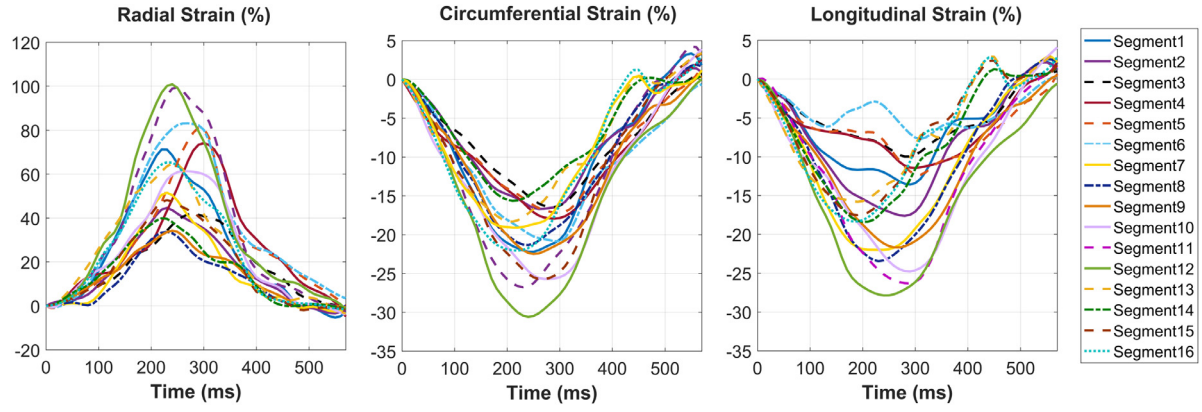

Fig. 2. Example of the three strain directions (radial, circumferential and longitudinal) of the 16 AHA segments of a single subject.

positive value. Fig. 2 shows the 16-radial strain time series of a single subject.

2.3. Attributes extraction using Principal Component Analysis

PCA is a statistical procedure that eliminates redundant data and condense the linearly uncorrelated information into a few variables called "principal components". The objective of applying PCA in this work is to reduce the spatial dimensionality while preserving the temporal information. The expression accounts for:

$$[Y]_{16\ \times\ 101} = [M]_{16\ \times\ 16} \times [X]_{16\times 101}$$

where Y is our data matrix for one subject (16 AHA-segments $\times$ 101 time points per segment), M corresponds to the transfer matrix and X to the source signals or components. The first few components (rows) of matrix X account for most of the variability. The transfer matrix represents the influence of the linear combination of the different principal components to each variable, so it gives information about the heterogeneity of the variables in terms of amplitude and shape of the time series. By analogy, this statement of the problem using PCA can be regarded as a source separation algorithm exploiting the information from the second order statistics, which can be computed via either eigenvalue decomposition or singular value decomposition, as detailed by Zarzoso and Nandi [30].

Accordingly, for each subject, PCA was performed on the 16 time-series of radial, circumferential and longitudinal strain (3 PCA analyses per subject) and the 16 coefficients of the transfer matrix associated to the 1st component (first column) were considered. For each of the three motion directions, the 16 coefficients were averaged to obtain three values per subject that summarized the global strain values.

2.4. Unsupervised clustering

To identify the patients with and without strain impairment, the SPSS Two-Step Cluster Component algorithm [16] in IBM SPSS (*version 23, SPSS Statistics/IBM Corp, Chicago II, USA*) was applied to the PCA 1st component coefficients of the patients' group. In brief, the first step of the algorithm pre-clusters the record into

many small sub-groups using a sequential clustering approach and then it clusters the sub-groups from the previous step, using the agglomerative hierarchical clustering method. It calculates then a proper number of clusters automatically identified [7]. To obtain the proper number of clusters, SPSS uses a two-step procedure that works well with the hierarchical clustering method: it calculates Bayesian information criterion for each number of clusters and then refines the initial estimate by finding the greatest change in distance between the two closest clusters [1]. The validation of consistency within clusters was done with the silhouette method, a value that ranges from −1 to +1, where a high value indicates that the object is well matched to its own cluster and poorly matched to neighboring clusters. So, if the silhouette value is high, the clustering configuration is appropriate [17].

2.5. Statistical differences between groups

A one-way ANOVA with a Bonferroni-corrected post-hoc analysis ($P = 0.05$) was performed to investigate the differences in normally distributed continuous variables between the different patients' groups and controls. Categoric variables were compared with the chi squared test or Fisher exact test, where applicable. A binomial logistic regression was constructed including in the model radial, circumferential and longitudinal strain PCA first components as independent variables. Accuracy, sensitivity and specificity of this model were compared with our supervised classification model. Boxplot and Receiver Operating Curves (ROC) representations were also performed. The statistical analysis was carried out with IBM SPSS Statistics for Windows, Version 23.0. Armonk, NY: IBM Corp.

2.6. Supervised classification

Supervised classification techniques require the definition of a class variable, in which each group has a different value. Each individual case was defined as a pattern vector of predictive variables: PCA 1st component coefficients of radial, circumferential and longitudinal strain. The aim was to build a model upon the data obtained in patients and controls in order to be able to classify a new subject into one of the groups according to their degree of strain impairment: severely impaired, mildly impaired and normal. Subsequently, a comparison with a model that classifies individuals in two categories, controls and patients was done. Naïve Bayes (NB) machine learning classification model [2] was used in this study, a simple classifier based on the Bayes Theorem. This classifier combines the prior probability (or previous experience) and the likelihood (based on the vicinity) to form a posterior probability using the Bayes' rule. The final classification is done taking the largest posterior probability. As Bayesian classifiers are usually based on categorical variables, NB was applied using supervised discretization to convert numeric attributes into nominal ones. To validate the performance of the model, 10-fold cross-validation [8] was applied. The construction of the classification model and its validation were performed with Weka explorer tools from Weka 3.8.1, University of Waikato, Hamilton, New Zealand [28].

To study the strain development in the evolutive dataset, the strain values (as the PCA 1st component coefficient) as a function of the time were first represented. Afterwards, the groups to which the new strain data belonged were predicted with the classification model previously built.

3. Results

3.1. Clinical and demographic features

The clinical and genetic characterization of the whole sample according to their level of LV strain impairment is presented in Table 1, whereas the clinical profile of the subset of patients with evolutive CMR images in the follow-up is provided in Table 2.

3.2. PCA results

The percentage of the total variance explained by the 1st principal component for each direction was (mean ± std): radial strain (controls: 95.20% ± 1.64%; patients: 90.55% ± 6.90), circumferential strain (controls: 96.19% ± 2.40%; patients: 93.59% ± 3.75%) and longitudinal strain (controls: 94.84% ± 2.43%; patients: 92.73% ± 4.94%).

3.3. Unsupervised clustering

The SPSS TwoStep Cluster Component algorithm detected two clusters in the patients' group. The quality of the cluster division was assessed with the silhouette measure, which was higher than 0.7 (1.0 states for the highest clustering performance). 40% of the patients (14 patients) were classified as Cluster 1, and showed a severe strain impairment (severely affected AC-LV patients) whereas 60% (21 patients) were classified as Cluster 2, and were patients with higher or close to normal strain values (mildly affected strain AC-LV patients).

3.4. Statistical differences between groups

There were statistically significant differences between groups for the PCA 1st component coefficients in all the motion directions as determined by one-way ANOVA tests: radial strain ($F(2,55) = 41.1$, $P < .001$); circumferential strain ($F(2,55) = 68.3$, $P < .001$) and longitudinal strain ($F(2,55) = 48.7$, $P < .001$). The Bonferroni post hoc tests revealed that all the comparisons were significant in all the motion directions (Fig. 3).

3.5. Supervised classification

3.5.1. NB classification model

Table 3 shows the NB classification rules. The strain rules with the best discrimination power among the strain groups were selected. The severely impaired strain group always showed a good concentration of individuals in the most unfavorable range of strain in the three directions. Conversely, the other two groups showed a significant crossover. Despite this overlap, the mildly impaired strain group mostly concentrated in a medium range of strains whereas the normal strain group was more heterogeneous, and its individuals allocated in the medium and the more favorable strain ranges in equal measures for each of the three directions.

The prediction obtained with the NB classification correctly identified as normal strain individuals 70% of the controls, as mildly impaired strain individuals 86% of mildly affected AC-LV patients and as severely impaired strain individuals as much as 100% of the severely affected AC-LV patients (Table 4), yielding an overall accuracy of 82.76% (100% for individuals with severely impaired strain).

The performance of the classifier, evaluated with a 10-fold cross validation technique, obtained an accuracy of 82.76%. Sensitivity, specificity, precision and F-measure for each group are shown in Table 5. Severely impaired strain group reached a 100% in all the metrics (all subjects were correctly classified), while normal strain group obtained the lowest values. The precision of the mildly impaired strain group was the lowest.

We aimed to match our PCA results against the more widely used methodology based on peak values. While the unsupervised clustering gave nearly the same results (only one patient changed its classification, from mildly affected with PCA to severely affected with peak values), the NB classifier obtained an accuracy of 68.96%

Table 1
Clinical, demographic and CMRI variables.

	Healthy controls (N=23)	*Mildly impaired patients (N=21)*	*Severely impaired patients (N=14)*	*p-value*
Age	49.6 ± 16.4	39.4 ± 19.9	39.4 ± 15.3	0.105
Sex (M/F)	10/13	10/11	7/7	0.921
Arterial hypertension	5	3	2	0.791
Diabetes mellitus	5	0	1	0.055
Ischemic heart disease	1	0	0	0.461
Dyslipemia	7	4	5	0.516
Mutated gene:				
-Desmoplakin	0	19 (90%)	10 (71%)	–
-Filamin C	0	1 (%)	0	–
-Desmin	0	0	1	–
-Plakophillin-2	0	1	0	–
-Transmembrane protein 43	0	0	2 (5.8%)	–
-Phospholamban	0	0	1	–
LGE distribution (%):				0.020[a,*]
Subepicardial	0	14 (67%)	7 (50%)	
Intramiocardial	0	3 (14%)	4 (29%)	
Both	0	4 (19%)	3 (21%)	
LVEDVi (ml/m²)	65.4 ± 14.9	68.8 ± 14.9	93.9 ± 19.4	<0.001*
LVEDVi >98ml/m² (%)	1 (4.3%)	1 (4.8%)	7 (50%)	<0.001*
LVESVi (ml/m²)	26.3 ± 9.0	31.8 ± 9.0	59.3 ± 16.0	<0.001*
LVEF (%)	60.5 ± 6.7	54.3 ± 4.5	37.5 ± 7.5	<0.001*
LVEF ≤55% (%)	5 (21.7%)	12 (57.1%)	13 (92.8%)	<0.001*
LV wall motion abnormalities † (%):				
-Presence	0	5 (23.8%)	6 (42.8%)	0.003*
-Location:				
Inferolateral	–	3	5	
Involving the anterior wall	–	2	1	
Peak strain (%):				
-Radial	42.8 ± 2.4	34.8 ± 1.2	18.6 ± 0.7	<0.001*
-Circumferential	−18.1 ± 0.6	−15.9 ± 0.3	−10.5 ± 0.3	<0.001*
-Longitudinal	−16.1 ± 0.4	−14.4 ± 0.3	−10.1 ± 0.5	<0.001*

[a] *Comparison between mildly and severely impaired strain patients since all the other p-values correspond to the comparison of the three clinical groups including controls.*
* *Denotes statistical significance with a p-value<0.050.*

Table 2
Clinical characterization of the evolutive dataset.

Sex	Subject1 Male	Subject2 Male	Subject3 Male	Subject4 Male	Subject5 Female	Subject6 Male
Age (B/F)	31/34	10/15	18/21	52/53	16/19	18/19
AC-mutated gene (additional VUS)	1 DSP	1 DSP	1 DSP (MYBPC3)	1 DSP (MYBPC3)	1 DSP	1 DSP
LGE (B/F)	Moderate, lateral and septum/Moderate, inferior, lateral and septum	No/mild, inferior	Severe, inferior, lateral and septum/Severe, inferior, lateral and septum	Severe, inferior, lateral and septum/Severe, inferior, lateral and septum	Moderate inferior and septum/Moderate inferior, lateral and septum	Moderate inferior and septum/Moderate inferior, lateral and septum
LVEF (B/F)	63/63	68/71	49/46	50/48	58/51	52/52
Enlarged LV (B/F)	No/No	No/No	Yes (LVEDVi 124 ml/m²)/Yes (LVEDVi 122 ml/m²)	Yes (LVEDVi 123 ml/m²)/Yes (LVEDVi 135 ml/m²)	No/No	No/No
LV Wall motion abnormalities (B/F)	No/No	No/No	Yes (inferior and lateral)/Yes (inferior and lateral)	Yes (inferior and lateral)/Yes (inferior and lateral)	Yes (inferior and lateral)/Yes (inferior and lateral)	No/No

Characterization of the six patients included in the evolutive dataset at baseline (B) and follow-up (F). VUS: variant of unknown significance.

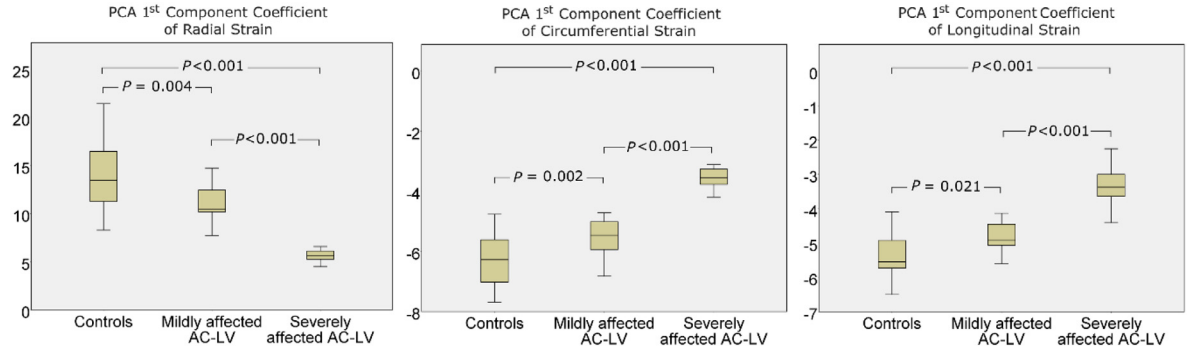

Fig. 3. Boxplots showing differences between groups with p-values obtained with the Bonferroni-corrected post-hoc analysis of the PCA 1st component coefficients of the radial, circumferential and longitudinal strain.

Table 3
NB classifier rules and % of patients in each range.

Attribute PCA 1st component coefficient of	Rules	Strain class		
		Normal ($N = 23$)	Mildly impaired ($N = 21$)	Severely impaired ($N = 14$)
Radial	[−inf,7.169]	0	0	**100**
strain	[7.169, 14.924]	**60.9**	**100**	0
(%)	[14.924,inf]	39.1	0	0
Circumferential	[−inf,-6.882]	34.8	0	0
Strain	[−6.882,4.458]	**65.2**	**100**	0
(%)	[−4.458,inf]	0	**0**	**100**
Longitudinal	[−inf,−5.459]	**65.2**	4.8	0
Strain	[−5.459,−4.075]	30.4	**95.2**	7.1
(%)	[−4.075,inf]	4.4	0	**92.9**

Results of the naïve Bayes classification rules applied to the whole sample (35 AC patients and 23 controls). In bold the higher percentage of subjects that belong to a certain range of strain values for each of the three strain groups.

Table 4
Confusion matrix of the strain NB classifier.

		Clinical group		
		Controls ($N = 23$)	Mildly affected AC-LV patients ($N = 21$)	Severely affected AC-LV patients ($N = 14$)
NB predicted strain classification	**Normal strain**	16	3	0
	Mildly impaired strain	7	18	0
	Severely impaired strain	0	0	14

Table 5
Classification performance of the NB strain classifier (3 groups).

Class	Sensitivity	Specificity	Precision	F-measure
Normal	0.696	0.914	0.842	0.762
Mildly impaired	0.857	0.811	0.720	0.783
Severely impaired	1.000	1.000	1.000	1.000
Weighted average	0.828	0.898	0.836	0.827

10-fold cross validation analysis of the NB classifier (Accuracy = 82.76%).

when applied to the clustering on peak strain values, well below the accuracy obtained with PCA of 82.76%.

The results of a NB classifier applied only to two groups, normal and altered strain, obtained a weaker accuracy of 75.86%. Notably, the performance of a standard procedure such as logistic regression modeling to predict the status of altered strain was slightly lower than that obtained with the NB classifier. The classification performances of both classifiers are summarized in Table 6.

Since LV-AC patients with severely affected strain were easily detectable with routine echocardiographic and CMR parameters, such as ventricular volumes and LVEF (Table 1), we now aimed to analyze the accuracy of the three strains to discriminate patients and controls in the grey zone, where the strain measurements are normal or only mildly impaired. Thus, ROC curves were constructed obtaining good Areas Under the Curve (AUC) ranging from 0.712 to 0.776 for the three strains, all of them statistically significant (Fig. 4). In keeping with the rationale of the Task Force Criteria, cut-off values at 100% specificity were selected even though their individual sensibility was rather low (Fig. 4).

3.5.2. Prediction of the evolutive dataset – a preliminary study

From the evolutive dataset obtained in six AC patients, the PCA 1st component coefficients corresponding to all three directions for each CMR acquisition were computed. For each subject, the evolution of these parameters as a function of time (in years) was represented, taking as a reference the year of the first CMR acquisition (Fig. 5). Regarding radial strain, all subjects exhibited a decrease. Specifically, the radial strain from two of these patients with fairly preserved values at the initial heart imaging decreased

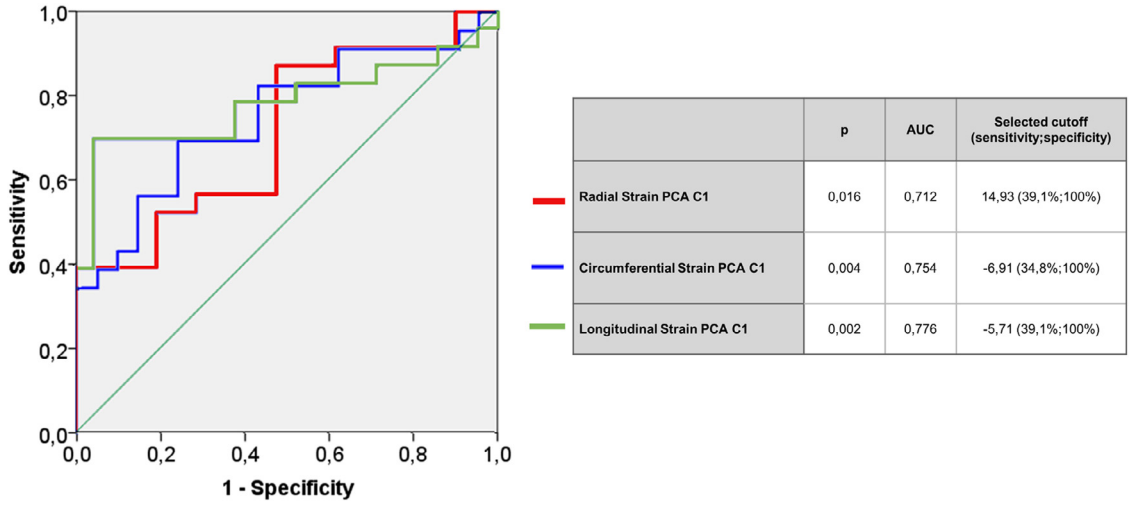

Fig. 4. ROC curves of radial, circumferential and longitudinal strain to discriminate between patients with moderate strain and controls, *p*-values, AUC and cutoff values.

Table 6
Classification performance from the NB/logistic regression strain classifier (2 groups).

Class	Sensitivity	Specificity	Precision	F-measure
Normal	0.696/0.609	0.800/0.806	0.696/0.667	0.696/0.636
Altered strain	0.800/0.806	0.696/0.609	0.800/0.763	0.800/0.784
Weighted average	0.759/0.729	0.737/0.685	0.759/0.726	0.759/0.726

10-fold cross validation analysis of the NB classifier (Accuracy = 75.86%) and logistic regression (Accuracy = 72.88%).

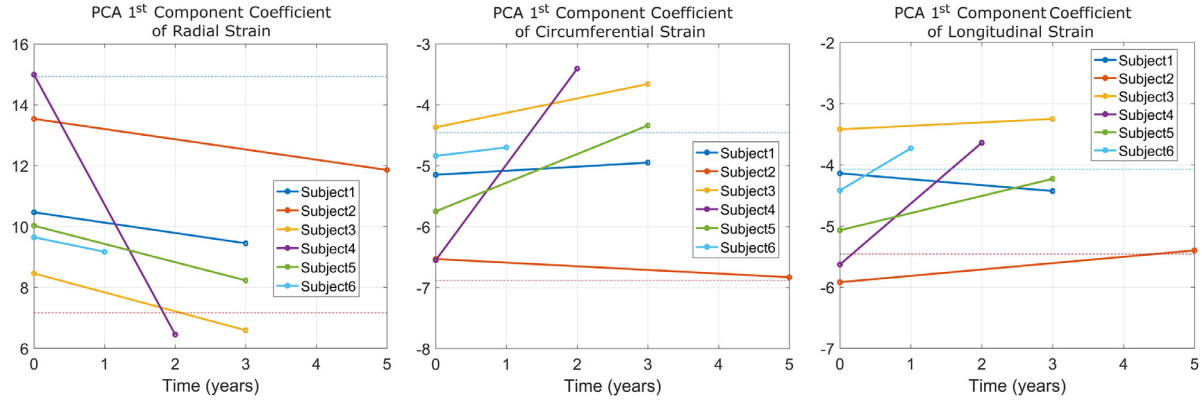

Fig. 5. PCA 1st component coefficient of the radial, circumferential and longitudinal strain of the evolutive dataset (six AC-LV patients) in time. *Dashed lines represent the thresholds of the NB model showed in Table 3.*

Table 7
Strain predictions of the NB classifier model using the evolutive dataset.

	Diagnosis at baseline	Diagnosis at follow-up	Years between CMR	Posterior probability
Subject 1	*Mildly impaired strain*	**Mildly impaired strain**	3	0.79
Subject 2	**Normal strain**	*Mildly impaired strain*	5	0.84
Subject 3	**Severely impaired strain**	*Severely impaired strain*	3	0.99
Subject 4	**Normal strain**	*Severely impaired strain*	2	0.84
Subject 5	*Mildly impaired strain*	**Severely impaired strain**	3	0.59
Subject 6	*Mildly impaired strain*	**Normal strain**	1	0.42

Predictions of the evolutive dataset, years between the CMRs and posterior probability associated to the predicted values. The diagnoses of the CMRs performed by the clustering algorithm and included in the model are showed in italics and the predictions performed by the NB model on the new data are showed in bold.

down to values that fell within the range corresponding to the severely impaired strain group output at the clustering stage.

Table 7 presents the diagnosis of the evolutive dataset at baseline and during follow-up, the years between both CMRs and the posterior probability associated to the predictions. Only the diagnoses marked in bold were predicted with the model, those in italics were obtained by clustering and used to build the NB model following the procedure described above. Both diagnoses (baseline and follow-up) were included in the table to better visualize the evolution of the patients.

According to Table 7, two patients did not change their strain classification (subjects 1 and 3), three patients got worse (subjects 2, 4 and 5) and one subject got better (subject 6). Regarding subject 6, the posterior probability associated to this prediction was quite small and therefore, not very reliable. As already appreciated in Table 5, the classifier performed worse for the individuals classified as normal strain and mildly impaired strain than for severely impaired strain.

4. Discussion

This work thoroughly characterizes the LV strain performance in the CMR of AC patients with LV involvement. Peak strain values depend on the sampling time of the acquisition, they are more susceptible to noise and fluctuation of the signal and they can also vary according to the interpolation method used. Moreover, when only the peak values are considered, relevant information related to the shape of the time series is unfortunately lost. To overcome these limitations the PCA methodology was applied to extract information from strain time series, thus reducing the dimensionality of the data to a few coefficients that consider both the amplitude and the shape of the series. In sum, it was found that found that: (1) 40% of the patients were severely affected, obtained by a clustering algorithm; (2) there were significant differences between controls, mildly and severely affected AC-LV groups and (3) a NB classifier could classify the degree of strain impairment to predict the clinical status in new cases, with an accuracy of 82.76% increasing up to 100% accuracy if the strain is severely impaired. (4) In our results, the NB classifier using the PCA approach outperformed the NB classifier with peak strain values (82.76% vs 69.96%), hence reinforcing our hypothesis that PCA should be preferred over peak values in this clinical scenario.

4.1. Sample characterization

As stated in the introduction, the diagnosis of AC relies on the fulfillment of certain TFC but obviously, not all the patients satisfy all the criteria included in the scoring system. Among AC patients, our clustering algorithm successfully classified 40% as patients with severely impaired strain and 60% as patients with better strain performance (without impairment or with mildly impaired strain). The ANOVA test detected significant differences between

all the groups, even between controls and mildly impaired strain patients. Thus, generally speaking, patients have lower radial and higher circumferential and longitudinal strain than controls, even those patients with more preserved strain values (Fig. 3). Remarkably, besides clear statistical differences in the comparisons no overlapping was observed between severely affected patients and the other two groups (Fig. 3).

4.2. Modelization and prediction of new cases

According to the NB model rules in Table 3, the individuals in the groups of severely and mildly impaired strain (95.2% to 100% and 92.9% to 100%, respectively) were mostly included within a single range of values. However, the normal strain group was more heterogeneous, ranging from mildly impaired to preserved strain values. Thus, as many as 60.9% (radial) and 65.2% (circumferential) of them overlapped with the mildly impaired strain group and only 39.1% (radial) and 34.8% (circumferential) were allocated in the most preserved range of values. The longitudinal rules were those which yielded a better discrimination power among clinical groups. The dispersion of the PCA 1st component coefficient of the radial strain values was very high compared to those of the circumferential and longitudinal strain. This effect was reflected in the thresholds associated to the rules in Table 3, graphically represented in Fig. 5 (dashed lines).

The classification performance after a 10-fold cross validation achieved a good classification accuracy (82.76%). However, although the model classifies extremely well the severely impaired strain individuals (100% classification accuracy), the normal and the mildly impaired strain groups were less iteratively reclassified in their respective categories (with sensitivities of 69.6% and 85.7%, respectively) (Table 5). The two-class classifier (normal vs altered strain) performed worse (accuracy of around 76% for NB classifier and around 73% for logistic regression) than the proposed three-class classifier due to the heterogeneity of the individuals in the most preserved strain categories (Table 6). In accordance with our previous report [27], the provided ROC curves with the three strains (Fig. 4) showed a good accuracy to discriminate patients and controls in a difficult clinical scenario when the routine LV volumes and function parameters fail to do it (Table 1). Indeed, all three strains showed a similar sensibility for a cutoff at 100% sensibility ranging from 34,8% and 39,1%. If replicated in other series with larger sample sizes and included in a future version of the Task Force Criteria, the implementation of LV strain analyses in CRM studies of patients with suspected AC could improve the performance of the current Task Force Criteria.

Finally, our brand-new study on the evolutive dataset in Fig. 5 revealed that disease progression affects more profoundly the radial strain than the strain in the other two directions. In the case of the circumferential and longitudinal strain, the progression was either milder or with a surprising slight improvement in the follow-up (one patient for each of those strain directions). This result suggests that radial strain measurements could be more robust and meaningful. Interestingly, in all the patients except for one (subject 4), the radial strain evolved with a similar and relatively smooth slope over time. Strikingly, subject 4 underwent a sharp decrease in all three directions. As seen in Table 2, this patient was the oldest of this subgroup with evolutive CMR data and in addition to his desmoplakin truncation he harbored a variant of uncertain significance in a sarcomeric gene that could have acted as a negative modifier (second genetic hit). Despite his bad strain evolution when the CMRs were performed (at the age of 52 and 53 years old), he did stay clinically stable in a NYHA class II until he reached 56, when he was recently admitted to hospital due to congestive heart failure with severe LV systolic dysfunction and listed for heart transplantation. Consistently, in the prediction phase, this subject was first diagnosed as a normal strain individual and moved to severely impaired strain individual in the second CMR acquisition with a quite high posterior probability (0.84). Subject 3, on the contrary, did not change much over time, however he was the patient with the most altered strain values and thus, he was diagnosed as a severely impaired strain individual in both CMRs. The remaining patients exhibited a slow evolution. Overall, strain measurements showed a consistent worsening with time even when no relevant changes were observed in the majority of the patients attending to the routine CMR report (Table 2). Focusing on this behavior, we put forward that these measurements could become clinically meaningful when the strain values drop down or go up to levels that undoubtedly refer to the severely impaired strain group.

The section related to global or regional dysfunction and structural alterations by CMR in the 2010 TFC [10] uses qualitative concepts, such as RV regional akinesia, dyskinesia and dyssynchronous contraction. Of note, the LV wall motion abnormalities are not considered and neither a precise threshold nor a measurement procedure for the RV assessment are provided. This work aims to underscore the potential of strain measurement to ascertain LV involvement in AC patients. If reproduced by other groups, it might be considered as an additional criterion for the diagnosis of AC with LV involvement at least in a clinical scenario as ours, where a pathogenic mutation and family involvement has been clearly identified. To that end, strain ranges for the different clinical groups as well as a classification model both to assign a strain and a clinical status with their sensibilities, specificities and respective accuracies was provided.

4.3. Extrapolation to RV analysis

As AC-RV cases are more frequently reported than AC-LV, the analysis of the RV dysfunction would also be highly valuable aiming to fine tune the current global and regional RV dysfunction criteria. However, the extrapolation of the methods described in this paper to the evaluation of the RV is still challenging. Firstly, it would require a widely accepted regional RV segmentation (analogously to the 17-region AHA segmentation of the LV). Furthermore, due to the reduced thickness of the RV, strain measurements on images obtained with the conventional CMR techniques would prove highly inaccurate. Therefore, new techniques and further research regarding the analysis of the RV strain in AC as well as in other cardiomyopathies is warranted.

4.4. Limitations of the study

We acknowledge that some limitations hamper the strain modelization in AC with LV in our study. The first one was the reduced sample size. Unfortunately, the enrollment of patients was limited by the low prevalence of the AC with LV involvement and the requirement of a positive genetic test to ensure the coherence of the diagnosis. The evolutive dataset was also very limited and explained by the fact that severe structural LV involvement usually lead to a cardioverter-defibrillator implantation which provoked distortion of cardiac imaging in subsequent CMR studies. The inclusion of more subjects and more acquisition time points will allow us to further characterize the fast and slow evolution patterns of AC patients with LV involvement. Finally, this assessment was faced from a family-based study where at least one member had a definite AC diagnosis and a mutation had been identified but, since AC can be suspected without such a robust familial and genetic background, comparative studies between LV strain parameters in AC patients and patients with other cardiomyopathies would be desirable.

Declaration of Competing Interest

The authors declare that they have no known competing financial interests or personal relationships that could have appeared to influence the work reported in this paper.

Acknowledgments

This work was supported by grants from the "Ministerio de Economía y Competitividad" [DPI2015-70821-R], "Instituto de Salud Carlos III" and FEDER "Union Europea, Una forma de hacer Europa" [PI14/01477, PI15/00748, PI18/01582, CIBERCV] and La Fe Biobank [PT17/0015/0043].

The study adheres the Declaration of Helsinki, was approved by the Comité Ético de Investigación Bioética, Hospital Universitario y Politécnico La Fe, and all subjects gave their informed consent to participate.

References

[1] J. Bacher, K. Wenzig, M. Vogler, SPSS TwoStep Cluster – A First Evaluation, Department of Sociology, Social Science Institute, Erlangen-Nuremberg, Germany, 2004 . Work and discussion paper.
[2] C. Bielza, P. Larrañaga, Discrete Bayesian network classifiers: a survey, ACM Comput. Surv. 47 (1) (2014) 1–43.
[3] M. Bourfiss, D.M. Vigneault, M. Aliyari Ghasebeh, B. Murray, C.A. James, C. Tichnell, F.A. Mohamed Howsein, S.L. Zimmerman, I.R. Kamel, H. Calkins, H. Tandri, B.K. Velthuis, D.A. Bluemke, A.S.J.M. te Riele, Feature tracking CMR reveals abnormal strain in preclinical arrhythmogenic right ventricular dysplasia/ cardiomyopathy: a multisoftware feasibility and clinical implementation study, J. Cardiovasc. Magn. Reson. 19 (1) (2017) 66.
[4] L. Breiman, Random forests, Mach. Learn. 45 (2001) 5–32 1.
[5] F. Castells, P. Laguna, L. Sörnmo, A. Bollmann, J. Millet, Principal Component Analysis in ECG Signal Processing, EURASIP J. Adv. Signal Process. 2007 (2007) 074580.
[6] G Cevenini, E. Barbini, M.R. Massai, P. Barbini, A naïve Bayes classifier for planning transfusion requirements in heart surgery: model for planning transfusions in heart surgery, J. Eval. Clin. Pract. 19 (1) (2013) 25–29.
[7] T Chiu, D. Fang, J. Chen, Y. Wang, C. Jeris, A robust and scalable clustering algorithm for mixed type attributes in large database environment, in: Proceedings of the Seventh ACM SIGKDD International Conference on Knowledge Discovery and Data Mining, ACM, New York, 2001, pp. 263–268.
[8] S Geisser, Predictive Inference: An Introduction, Chapman & Hall, New York, 1993 264.
[9] B Igual, E. Zorio, A. Maceira, J. Estornell, M.P. Lopez-Lereu, J.V. Monmeneu, A. Quesada, J. Navarro, F. Mas, A. Salvador, Arrhythmogenic cardiomyopathy. Patterns of ventricular involvement using cardiac magnetic resonance, Rev. Esp. Cardiol. 64 (12) (2011) 1114–1122.
[10] F.I. Marcus, W.J. McKenna, D. Sherrill, C. Basso, B. Bauce, D.A. Bluemke, H. Calkins, D. Corrado, M.G.P.J. Cox, J.P. Daubert, G. Fontaine, K. Gear, R. Hauer, A. Nava, M.H. Picard, N. Protonotarios, J.E. Saffitz, D.M. Yoerger Sanborn, J.S. Steinberg, H. Tandri, G. Thiene, J.A. Towbin, A. Tsatsopoulou, T. Wichter, W. Zareba, Diagnosis of arrhythmogenic right ventricular cardiomyopathy/dysplasia: proposed modification of the task force criteria, Eur. Heart J. 31 (7) (2010) 806–814.
[11] W.J. McKenna, G. Thiene, A. Nava, F. Fontaliran, C. Blomstrom-Lundqvist, G. Fontaine, F. Camerini, Diagnosis of arrhythmogenic right ventricular dysplasia/cardiomyopathy, Br. Heart J. 71 (3) (1994) 215–218.
[12] D.A. Morales, Y. Vives-Gilabert, B. Gómez-Ansón, E. Bengoetxea, P. Larrañaga, C. Bielza, J. Pagonabarrage, J. Kulisevsky, I. Corcuera-Solano, M. Delfino, Predicting dementia development in Parkinson's disease using Bayesian network classifiers, Psychiatry Res. 213 (2) (2013) 92–98.
[13] S. Narula, K. Shameer, A.M. Salem Omar, J.T. Dudley, P.P. Sengupta, Machine-learning algorithms to automate morphological and functional assessments in 2d echocardiography, J. Am. Coll. Cardiol. 68 (21) (2016) 2287–2295.
[14] K. Pearson, On lines and planes of closest fit to systems of points in space, Philos. Mag. 2 (1901) 559–572.
[15] G. Prati, G. Vitrella, G. Allocca, D. Muser, S.C. Buttignoni, G. Piccoli, G. Morocutti, P. Delise, B. Pinamonti, A. Proclemer, G. Sinagra, G. Nucifora, Right ventricular strain and dyssynchrony assessment in arrhythmogenic right ventricular cardiomyopathy: cardiac magnetic resonance feature-tracking study, Circ. Cardiovasc. Imaging 8 (11) (2015) e003647 discussion e003647.
[16] edited by L. Rokach, O. Maimon, Clustering methods, in: O. Maimon, L. Rokach L. Boston: (Eds.), Data Mining and Knowledge Discovery Handbook, Springer, US, 2005, p. 321—52. edited by.
[17] P.J. Rousseeuw, Silhouettes: A graphical aid to the interpretation and validation of cluster analysis, J. Comput. Appl. Math. 20 (1987) 53–65.
[18] S. Sen-Chowdhry, P. Syrris, D. Ward, A. Asimaki, E. Sevdalis, W.J. McKenna, Clinical and genetic characterization of families with arrhythmogenic right ventricular dysplasia/cardiomyopathy provides novel insights into patterns of disease expression, Circulation 115 (13) (2007) 1710–1720.
[19] S. Sen-Chowdhry, P. Syrris, S.K. Prasad, S.E. Hughes, R. Merrifield, D. Ward, D.J. Pennell, W.J. McKenna, Left-dominant arrhythmogenic cardiomyopathy, J. Am. Coll. Cardiol. 52 (25) (2008) 2175–2187.
[20] S. Sen-Chowdhry, R.D. Morgan, J.C. Chambers, W.J. McKenna, Arrhythmogenic cardiomyopathy: etiology, diagnosis, and treatment, Annu. Rev. Med. 61 (1) (2010) 233–253.
[21] P.P. Sengupta, Y.M. Huang, M. Bansal, A. Ashrafi, M. Fisher, K. Shameer, W. Gall, J.T. Dudley, Cognitive machine-learning algorithm for cardiac imaging: a pilot study for differentiating constrictive pericarditis from restrictive cardiomyopathy, Circ. Cardiovasc. Imaging 9 (6) (2016) e004330, doi:10.1161/CIRCIMAGING.115.004330.
[22] O.A. Smiseth, H. Torp, A. Opdahl, K.H. Haugaa, S. Urheim, Myocardial strain imaging: how useful is it in clinical decision making? Eur. Heart J. 37 (15) (2016) 1196–1207.
[23] M. Tabassian, M. Alessandrini, L. Herbots, O. Mirea, E.D. Pagourelias, R. Jasaityte, J. Engvall, L.D. Marchi, G. Masetti, J. D'hooge, Machine learning of the spatio-temporal characteristics of echocardiographic deformation curves for infarct classification, Int. J. Cardiovasc. Imaging 33 (8) (2017) 1159–1167.
[24] S. Theodoridis, K. Koutroumbas, in: Pattern Recognition, Elsevier Acad. Press, Amsterdam, 2009, p. 984.
[25] L.F. Tops, K. Prakasa, H. Tandri, D. Dalal, R. Jain, V.L. Dimaano, D. Dombroski, C. James, C. Tichnell, A. Daly, F. Marcus, M.J. Schalij, J.J. Bax, D. Bluemke, H. Calkins, T.P. Abraham, Prevalence and pathophysiologic attributes of ventricular dyssynchrony in arrhythmogenic right ventricular dysplasia/cardiomyopathy, J. Am. Coll. Cardiol. 54 (5) (2009) 445–451.
[26] V. Vapnik, in: The Nature of Statistical Learning Theory, Springer, New York, 2000, p. 314.
[27] Y. Vives-Gilabert, J. Sanz-Sánchez, P. Molina, A. Cebrián, B. Igual, P. Calvillo–Batllés, D. Domingo, J. Millet, L. Martínez-Dolz, F. Castells, E. Zorio, Left ventricular myocardial dysfunction in arrhythmogenic cardiomyopathy with left ventricular involvement: a door to improving diagnosis, Int. J. Cardiol. 274 (2019) 237–244.
[28] I.H. Witten, E. Frank, in: Data Mining: Practical Machine Learning Tools and Techniques, Elsevier, Amsterdam, 2017, p. 525.
[29] K.C.L. Wong, M. Tee, M. Chen, D.A. Bluemke, R.M. Summers, J. Yao, Regional infarction identification from cardiac CT images: a computer-aided biomechanical approach, Int. J. Comput. Assist. Radiol. Surg. 11 (9) (2016) 1573–1583.
[30] edited by V. Zarzoso, A.K. Nandi, Blind source separation, in: A.K. Nandi. (Ed.), Blind Estimation Using Higher-Order Statistics, Kluwer Academic Publisher, Boston, 1999, pp. 167–252. edited by.